applied sciences

MDPI

Article

Experimental Evaluation of a Solar Low-Concentration Photovoltaic/Thermal System Combined with a Phase-Change Material Cooling Technique

Mahmoud B. Elsheniti [1,2,*], Saad Zaheer [1], Obida Zeitoun [1,3], Hassan Alshehri [1], Abdulrahman AlRabiah [1] and Zeyad Almutairi [1,3]

[1] Department of Mechanical Engineering, College of Engineering, King Saud University, Riyadh 11451, Saudi Arabia
[2] Mechanical Engineering Department, Faculty of Engineering, Alexandria University, Alexandria 21544, Egypt
[3] K.A.CARE Energy Research and Innovation Center, King Saud University, Riyadh 11451, Saudi Arabia
* Correspondence: mbadawy.c@ksu.edu.sa

Abstract: The high operating temperatures of photovoltaic (PV) panels negatively affect both electrical efficiency and material degradation rate. Combining both a water-cooling-based photovoltaic/thermal (PV/T) system and a phase-change material (PCM) with/without low concentration (LC) represents a promising solution for boosting the overall energy conversion efficiency of the PV system. This approach needs to be evaluated in harsh weather where the PCM should have a high melting temperature. Therefore, this study experimentally investigates the performance of three PV cooling systems, namely PV-PCM, PV/T-PCM, and LCPV/T-PCM, compared to a reference PV without cooling, under the weather conditions of Riyadh. The results show that the PV/T-PCM attained the highest daily average electrical and overall efficiencies of 14.24% (5% increase) and 42.7%, respectively, compared to 13.56% electrical efficiency of the reference panel. The electrical efficiency of the PV-PCM was 13.64% due to inefficient natural cooling in the afternoon. The LCPV/T-PCM recorded the best performance during the two hours around noon, with an average increase in electrical power and efficiency of 11.06% and a maximum overall efficiency of 70%. Finally, the LCPV/T-PCM system can be only effectively used to support the higher demand for electricity and thermal energy around noon; otherwise, a new design configuration with low concentration is needed to establish a higher electrical efficiency in most hours of sunlight.

Keywords: photovoltaic cooling; photovoltaic efficiency; solar low concentration; phase change material; high ambient temperature

Citation: Elsheniti, M.B.; Zaheer, S.; Zeitoun, O.; Alshehri, H.; AlRabiah, A.; Almutairi, Z. Experimental Evaluation of a Solar Low-Concentration Photovoltaic/Thermal System Combined with a Phase-Change Material Cooling Technique. *Appl. Sci.* **2023**, *13*, 25. https://doi.org/10.3390/app13010025

Academic Editor: Luis Lugo

Received: 23 November 2022
Revised: 10 December 2022
Accepted: 19 December 2022
Published: 20 December 2022

1. Introduction

In recent years, Saudi Arabia's energy utilization has been a significant indicator of its financial progress. The requirement for energy has become one of the most significant parts of the country's development and growth. However, electric energy production has become the biggest concern worldwide, mainly due to the increase in the cost of fossil fuels, politically-driven energy markets, environmental aspects, global warming, and the accessibility of fossil fuels versus demand. In 2030, energy utilization in Saudi Arabia is anticipated to rise by 365.4 terawatt hours (TWh), as reported by reference [1]. The Ministry of Energy is working on expanding the national energy utilization in power generation, increasing the share of natural gas and renewable energy sources to roughly 50% by 2030 while diminishing the use of fossil fuels through the National Renewable Energy Program (NREP) [2]. In 2020, 63.1% of the Kingdom's annual electricity generation was gas based, whereas 36.7% was oil-based electricity generation [3]. This has driven a lot of researchers and scientists to consider the possibility of making amends for the energy

generated by fossil fuels with unconventional, economic, and renewable resources to meet the anticipated gigantic increase in energy demand by 2030. Among such resources, solar energy has been found to be an auspicious resource of renewable energy in the Kingdom [4].

Photovoltaic panels retain a significant amount of solar energy. However, only a tiny portion of the solar irradiance contributes to the direct transformation of energy into valuable energy, whereas 75–80% of it is disseminated as waste heat, and around 4–8% is reflected. Roughly 8–20% of solar energy is converted into electricity [5]. The remaining portion of solar energy is converted into heat, which causes the solar cells to overheat. The surface of PV panels can heat up to temperatures above ambient [6]. This increase in temperature caused by solar-cell heating reduces the electrical efficiency of PV panels. PV panel conversion efficiency decreases by 0.4% to 0.65% for every degree increase in PV cell temperature [7]. Radziemska [5] concluded that the electrical efficiency of PV panels falls by 0.08% for every increment in the temperature of the PV panels, thus diminishing the power output of the PV panels by 0.65%. Therefore, cooling PV panels by utilizing appropriate cooling strategies is essential for efficiency improvement and economic aspects. Researchers have proposed numerous cooling approaches. These cooling strategies are classified into two categories: active cooling systems and passive cooling techniques. PV panel temperature can be controlled by utilizing phase-change materials (PCMs) as a passive cooling method. PCMs will absorb thermal energy from PV panels needed for their phase change from the solid to the liquid phase to maintain the panels at low temperatures, preventing drastic drops in voltage and efficiency. Moreover, PV panels utilizing PCMs (PV-PCM) do not require any additional power source to run the system.

The PCM in a PV-PCM module absorbs heat and lowers the panel's temperature. Stropnik and Stritih [8] reported that the power generated by a PV module can be enhanced by approximately 9.2% at a maximal solar irradiance of 571 W/m^2 by incorporating RT28HC PCM on the backside of the panel. Rajvikram et al. [9] deployed PV-PCM panels that had aluminum sheets attached to the backside of the modules as part of an experimental investigation. They demonstrated that the PCM could enhance power efficiency by an average of 2.2%, while dropping the PV module temperatures by an average of 4.4 °C [10]. Nada et al. [11] investigated experimentally the variation of PV panel efficiency and temperature for three PV-PCM cooling cases. They found that the PV temperature decreased 10.6 °C when employing a PCM-AL2O3 nanoparticle compound. Baygi and Sadrameli [12] used Polyethylene glycol 1000 as a PCM to cool PV panels. They investigated the effect of using this PCM on the PV efficiency at different panel slope (0° and 15°). They observed that the temperature of the panel cooled by the PCM decreased about 15 °C and its power output increased by 8%. Huang et al. [13] carried out experimental and numerical studies to investigate the cooling effect of using a stable paraffin (ZDJN-28)/Expanded graphite composite on PV performance. The results of [13] indicated that the maximum temperature of a PV-PCM panel decreased by 4.7 °C, and the suitable density of the PCM to achieve high-temperature management performance was 900 Kg/m^3. Bilgin et al. [14] studied the effect of PCMs from an economical perspective and conducted numerical studies under two Turkish cities' climate conditions. They reported that using PCM cooling decreased the PV panel temperature by 10.26 °C, increased the efficiency by 0.48–3.73%, and improved the average annual efficiency by 1.59%.

Wongwuttanasatian et al. [15] examined experimentally the performance of three 20W PV panels cooled by using three different configurations of PCM containers. They reported a 5.3% enhancement in electrical efficiency when they applied a finned container filled with Palm wax-based PCM. They also noticed that the PCM may not be effective in late afternoon with irradiance lower than 500 W/m^2. Karthick et al. [16] studied experimentally the performance of a building-integrated photovoltaic cooled by a Glauber's salt-based PCM with a 32 °C melting point, which is close to the ambient temperature of the experimental location in India. They reported a 10% increase in electrical efficiency resulting from a reduction in the PV surface temperature of up to 8 °C, compared to a reference PV. Reddy et al. [17] investigated the depth of a PCM's container required for the optimal PCM

quantity under different operating conditions. They reported that an increase in the ambient temperature of 8 °C required an increase in PCM tank depth by 1.7 cm, and a large amount of PCMs with a low-melting temperature, i.e., near ambient temperature. A hybrid PV cooling system was introduced by Yang et al. [18] where a PCM container was integrated into a photovoltaic/thermal (PV/T) system. Compared to the conventional PV/T system, the data of [8] revealed that the PV maximum-temperature drop for the PV/T-PCM system reached 15.8 °C and the output power increased by 7.4 W. This examination was for a PCM with a transition temperature of 30 °C, which cannot be used with a higher ambient temperature, such as in Riyadh. Elsheniti et al. [19] proposed a mathematical model for predicting the performance of a PV panel cooled by a PCM with a melting temperature of 25 °C. They noticed that the passive strategies were insufficiently effective to guarantee adequate cooling. The PCM was only able to ensure adequate cooling for the first few hours, and it was only able to reduce the module's operating temperature, on average, for certain period of the day. As soon as the melting was finished, the PCM ceased to function, which caused the panel temperature to quickly increase to a point where it exceeded that of the uncooled panel.

Numerous studies on active cooling techniques have been conducted in this area to enhance PV electrical efficiency by regulating the temperature of PV panels in hot climate regions. Bahaidarah [20] used a jet cooling approach under a PV panel and reported maximum temperature drops of 33.1 °C and 16.5 °C for June and December, respectively, under the hot weather conditions of Dhahran, Saudi Arabia. Using water directly to cool PV panels requires makeup water, and this will increase in dry weather conditions. Additionally, pumping power is required which should be evaluated to determine the net advantage of such approaches. Teo et al. [21] carried out an experiment to investigate the efficiency of PV panels with and without active cooling. Without active cooling, they discovered that the module's temperature was high, and the efficiency of the solar cells was in the range of 8–9%. Meanwhile, the temperature of the PV was diminished significantly when the module was cooled by forced convection, leading to an increase in the efficiency by 12% to 14%. In another experiment by Parupudi et al. [22], they indicated that, when compared to an asymmetric compound parabolic concentrator (ACPC) with no cooling impact, the total energy output and the conversion efficiency of an ACPC with active cooling was enhanced by 31%.

Although active cooling techniques have better cooling efficiency, the energy needed to operate the cooling equipment, and the high cooling-equipment operating and maintenance costs may prevent them from being applied to large-scale solar power plants. To minimize the levelized cost of energy, integration of passive cooling with active cooling can result in a better solution where waste thermal energy can also be utilized to support other applications, such as a thermal membrane distillation [23]. Therefore, the main goal of this research is to experimentally assess the impact of using a passive−active cooling strategy to maintain a PV panel's optimal operating temperature and improve the overall solar energy conversion efficiency, under the environmental conditions of Riyadh, KSA. The current investigation is based on the performance comparison of four PV panels installed in the same location. The first one is used as a reference without any cooling approach, the second is a PV-PCM system, the third is a combined passive−active cooling system (PV/T-PCM), and the fourth is an integration of low solar-concentration sheets to the PV/T-PCM (LCPV/T-PCM). In most of the previous studies on PV cooling using PCMs, the phase transition temperatures were in the range of 25–30 °C for different PCMs. In the current study, the ambient high-temperature conditions of Riyadh city are considered in evaluating the proposed hybrid systems. Therefore, new experimental data are explored and discussed to compare and examine the workability of integrating these systems with a PCM with a high transition temperature of 41–48 °C.

2. Materials and Methods

The experimental system layout, as shown in Figure 1, consists of four 120W monocrystalline photovoltaic panels [24]; eight solar batteries (Gel Battery, 12V); two batteries each connected in series to obtain 24 V [25]; a 120W DC floodlight as an electric load for discharging the batteries; four PWM solar charge controllers [26]; an OMB data logger [27]; seventeen BST-TP01 [28] thermocouples; a pyranometer [29]; a multimeter [30]; a PV analyzer (PROVA 200A) [31]; a 0.15 HP pump; and a 100 L tank. Figure 2 shows the on-site experimental facilities, including the PV panels, loads, and control and measuring devices.

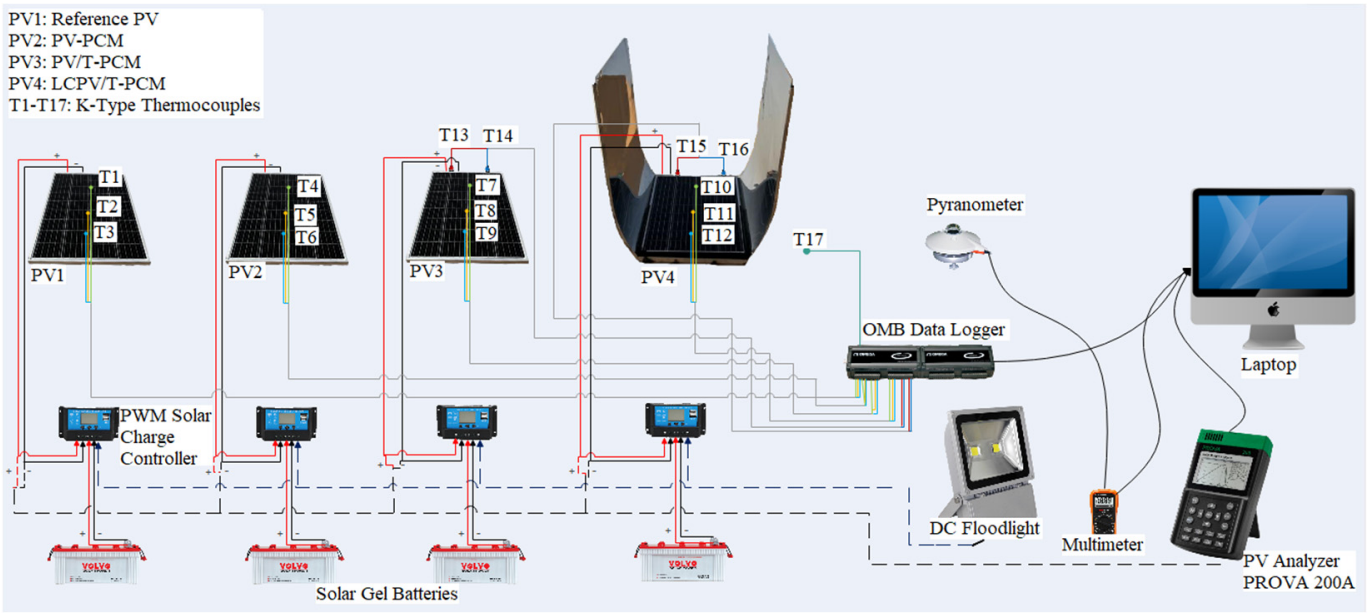

Figure 1. Schematic diagram of the system.

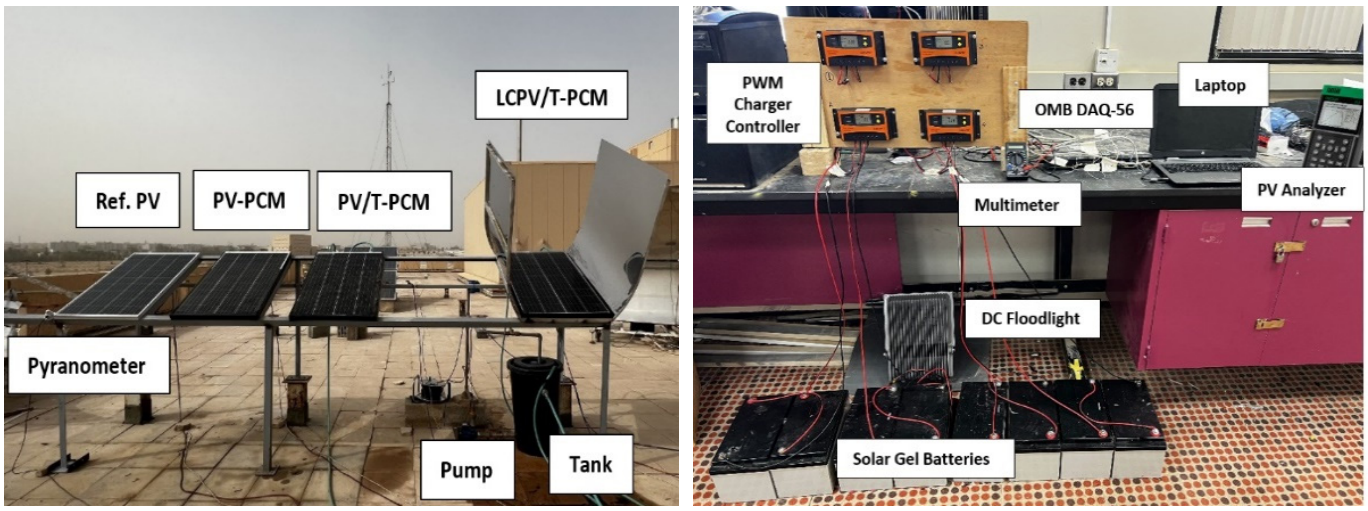

(**a**) (**b**)

Figure 2. Pictorial views of the experimental layout: (**a**) outdoor facilities, and (**b**) indoor load, control, and measuring devices.

The following are the descriptions of the components used in the experimental setup and approaches for the design or selection of each one.

PV panels: Four identical monocrystalline Maysun solar PV panels with an area of 0.694 m^2 each were purchased from the local market due to their availability and cost [24]. The specifications of the opted PV panels are given below in Table 1.

Table 1. Specifications of the PV panels used in the experimental tests [32].

Model No.	Rated Maximum Power	Tolerance	Voltage at Pmax	Current at Pmax	Open Circuit Voltage	Short Circuit Current	Normal Operating Cell Temp.	Operating Temp.	Dimension
MS120M-36	120 W	0~+5%	18.2 V	6.67 A	21.51 V	7.19 A	47 ± 2 °C	−40 to +85 °C	1020 × 680 × 30 mm

PCM selection: The experimental study was conducted at King Saud University in Riyadh, KSU, where the average ambient temperature is above 40 °C throughout the summer season. Therefore, the PCM melting temperature should be greater than the recorded ambient temperature of the location to stay in a solid phase. Consequently, the PCM subjected to the ambient air will perform its function only when the PV panel has a temperature higher than ambient. The PCM should also have high latent heat to maintain the PV panel's temperature around the melting point as long as possible. The second reason to consider a relatively high PCM melting temperature is to recover heat at a relatively high temperature when applying the combined passive−active approach in this study. Hence, Rubitherm RT-47 [32] was the best option for the current investigation based on its melting point temperature, which matches the ambient temperature in Riyadh. In addition, it has acceptable thermophysical properties that can lead to a better performance for the current system. The specifications of the obtained PCM are given in Table 2.

Table 2. The specifications of the RT-47 PCM used in the present work [32].

Melting Point	Heat Storage Capacity ±7.5%	Specific Heat Capacity	Density Solid at 15 °C	Density Liquid at 80 °C	Heat Conductivity (Both Phases)	Volume Expansion	Flash Point	Max Operating Temp.
41–48 °C	160 kJ/kg	2 kJ/kg K	0.88 kg/L	0.77 kg/L	0.2 W/m k	12%	>180 °C	65 °C

Tube configuration: A copper tube with an outer diameter of 12.5 mm and an inner diameter of 10.4 mm was designed in a U-bend rectangular shape to cover the whole back side of the PV. The pipe configuration was made from one piece without any use of external fittings.

LCPV design: The operation of PV cells under concentrated irradiance offers two main advantages: First, fewer solar cells are needed due to the objectification of an optic system to concentrate incident irradiance from the sun onto a smaller area of conventional solar cells. Second, the increase in the solar irradiation density incident on the PV cells increases their electrical output. A challenge in LCPV is the design and construction of an optical system that creates an invariant radiation profile. The electrical performance of PV cells is largely dependent on the uniformity of the solar irradiance profile, as non-uniform irradiance may lead to PV cell mismatch as well as power loss. The design of the LCPV is shown in Figure 3 and described by the following equations [33].

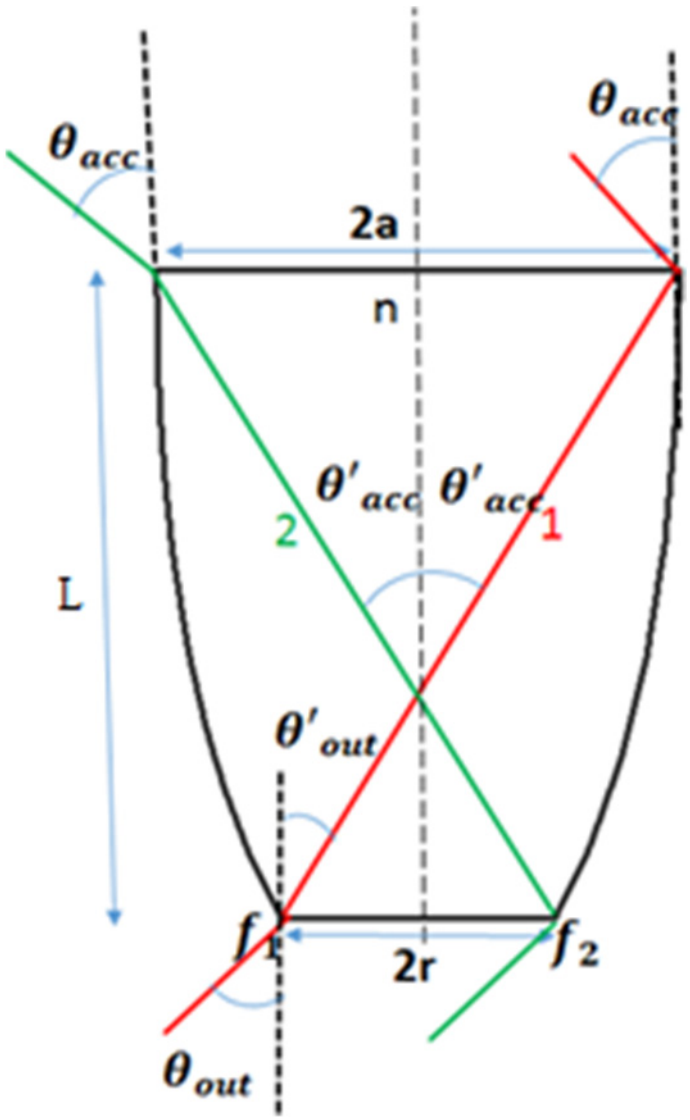

Figure 3. LCPV cross-sectional view.

$$a = n\frac{r}{sin\theta_{acc}} \tag{1}$$

$$L = (a + r)\ cot\theta'_{acc} \tag{2}$$

$$f = \frac{r(sin\theta_{out} + sin\theta_{acc})}{n} \tag{3}$$

$$\theta'_{acc} = 2across\frac{1}{n} - \theta'_{out} \tag{4}$$

where a is the input radius; r is the exit radius; L is the LCPV length; θ_{out} and θ'_{out} are the external and internal output angle, respectively; and θ_{acc} and θ'_{acc} are the external and internal acceptance angle, respectively.

Reference PV (PV1): For PV1, the PV panel obtained from the market was used without modifications as a reference PV panel, and three BST-TP01 K-type thermocouples were fixed at the middle line of the PV panel's back and used to measure the back surface temperature. Similarly, three thermocouples were fixed at the same position on the back of each of the other three panels. The average of the readings of the three thermocouples was considered to represent the PV temperature.

PV-PCM (PV2): In this case, after fixing the thermocouples, the back side of the PV2 panel was filled with 12.5 kg of Rubitherm RT-47 PCM, as shown in Figure 4a. Then, it was completely sealed from the back with an acrylic sheet of 5 mm thickness.

(**a**) (**b**) (**c**) (**d**)

Figure 4. Pictorial views of equipping the PV panels with PCM and LCPV: (**a**) PV2, (**b**) PV3, (**c**) PV4, and (**d**) PV4 with low-concentrator.

PV/T-PCM (PV3): Here, after fixing the thermocouples, a copper tube coil in rectangular shape was fixed to the back surface of the panel, assuring a good contact to eliminate the thermal contact resistance as shown in Figure 4b. Then, 11 kg of Rubitherm RT-47 was used to fill the back of the panel. After that, an acrylic sheet of 10 mm was used to cover the opening.

LCPV/T-PCM (PV4): The panel is identical to the PV3 panel as shown in Figure 4c, but a low-concentration frame was designed for this case and fixed in the frame structure of the system, as shown in Figure 4d.

The performance of the PV panels in this study are expressed by the instant electrical power and the daily average electrical and overall efficiencies. The maximum electrical power output that could be generated from each PV panel was traced by the PV analyzer and recorded every 10 min. The PV analyzer applied a load on the PV panels for a few seconds to record the maximum power, while the solar batteries were connected to the PV panels to ensure continuous loading on the panels over the day. The typical equation used to calculate the daily average electrical efficiency can be written as follows:

$$\eta_{electrical} = \frac{P_{electrical}}{I\ A} \tag{5}$$

where $P_{electrical}$ and I are the daily average electrical power and solar irradiance over the investigated period, respectively, while A is the panel area. The PV3 and PV4 panels also provide thermal power output that can be used to drive an external system. Therefore, the daily average thermal and overall efficiencies of the PV3 and PV4 panels can be written as follows [34,35]:

$$\eta_{thermal} = \frac{\dot{m}_w\ c_{pw}\ (T_e - T_i)}{I\ A} \tag{6}$$

$$\eta_{overall} = \eta_{electrical} + \eta_{thermal} \tag{7}$$

where $\dot{m}_w$ is the thermal fluid mass flow rate; c_{pw} is the specific heat capacity of the thermal fluid; and T_i and T_e are the inlet and exit temperatures of the thermal fluid. The water pump was operated from the grid as it was used for both the PV3 and PV4 panels, and its power consumption was not considered in the performance evaluation.

Table 3 depicts the details of the instruments used in the experimental tests. The uncertainty in the performance parameters is calculated based on the given information in Table 3 for the independent readings and according to Equation (8) [36]. The uncertainty in each of the performance parameters is summarized in Table 4. Since electrical power is directly taken from the PV analyzer, accordingly, its uncertainty is ±1%. The uncertainties of the electrical and overall efficiencies are ±0.004 (±2.8% of the efficiency value) and ±0.0344 (±8% of the efficiency value), respectively. These uncertainties were calculated based on the daily average experimental data of Day 3 of the PV/T-PCM, where the average inlet and outlet temperatures were 23.09 ± 0.84 °C and 24.16 ± 0.91 °C, respectively, and average solar irradiance was 730.68 W/m^2. The five days were in the same month where the averages recorded for the minimum and maximum solar irradiance were 730.68 W/m^2 on Day 3 and 774.4 on Day 5, respectively. The average measured minimum and maximum inlet cooling temperatures were 20.38 °C on Day 1 and 23.64 °C on Day 5, respectively. The variation in the ambient temperatures is shown in Figure 5a, which is limited to a maximum of 3 °C or 4 °C at each given time. These close experimental conditions make some kind of verification of the results and using the data of Day 3 to calculate the uncertainty seems reasonable.

$$w_R = \left[\left(\frac{\partial R}{\partial x_1} w_1 \right)^2 + \left(\frac{\partial R}{\partial x_2} w_2 \right)^2 + \cdots + \left(\frac{\partial R}{\partial x_n} w_n \right)^2 \right]^{\frac{1}{2}} \quad (8)$$

Table 3. The models' name and accuracy of the apparatus used in the experimental setup.

Apparatus	Model Name	Accuracy
Pyranometer	HUKSEFLUX–LP02	<±1% (100–1000 W/m^2)
PV Analyzer	PROVA-200A	±1%
Thermocouples (K-Type)	BESANTEK–BST TP01	±0.4 %
Solar Controller	EURONET-10A	±1%
Gel Batteries	EURONET-EUR6512 (65AH)	–
Pump	HYUNDAI-HWP0024 (0.15HP)	–
Floodlight (DC 12-24V)	SHAHPAN-GRTGDY 120W	–

Table 4. The uncertainty in the performance parameters.

Parameter	Uncertainty Value	Uncertainty Percentage
Electrical power	0.722 W	±1%
Electrical efficiency	±0.004	±2.8%
Overall efficiency	±0.0344	±8%

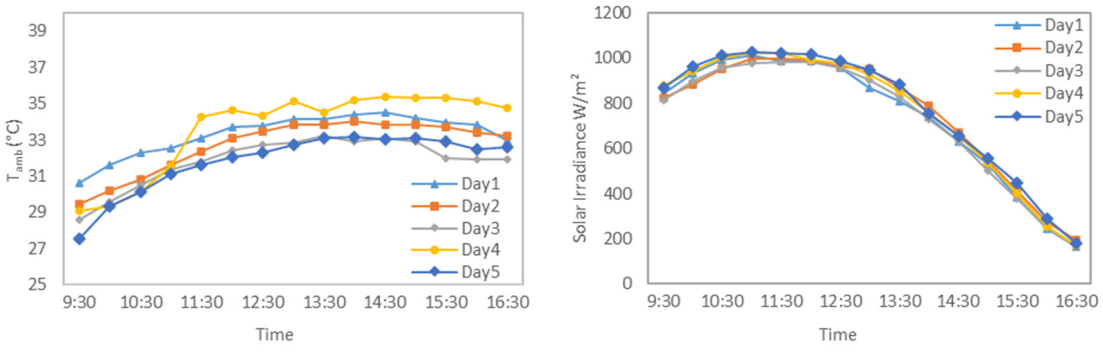

Figure 5. The weather conditions during five days in October 2022 in Riyadh from 9:30 to 16:30: (**a**) ambient temperature, and (**b**) total solar irradiance.

3. Results and Discussion

The electrical and thermal performances of the four PV panels were experimentally evaluated during the days of 12, 13, 15, 16, and 17 October 2022 at the Mechanical Engineering Department, Kind Saud University, Riyadh, KSA. The ambient temperature and total irradiance at the same inclination angle of the PV panels are depicted in Figure 5, for the five investigated days from 9:30 to 16:30. The average ambient temperatures of Day 1 to Day 5 were 33.36 °C, 32.69 °C, 31.87 °C, 33.54 °C, and 31.77 °C, respectively, while the average irradiances were 739.53 W/m^2, 754.77 W/m^2, 730.68 W/m^2, 760.58 W/m^2, and 774.37 W/m^2 for the five days, respectively. The recorded average ambient temperature in October was moderate compared to the average maximum temperature of 43 °C in August, while the solar irradiance in October was the highest over the year in Riyadh. This condition helped in examining the effect of the melting temperature of the PCM that was selected for the summer season on the PV performance in other seasons. In addition, the reference PV (PV1) panel was not surrounded by a higher ambient temperature which allowed natural cooling to play a role in managing the PV1 panel's temperature. Although the speed and direction of the surrounding air might affect the results, the simultaneous comparison of the four PV panels at the same location made the comparison independent of the air movement.

The mass flow rates of the circulated cooling water at the back of the PV/T-PCM (PV3) and the LCPV/T-PCM (PV4) were identical on the same day. They were 0.3703, 0.96246, 1.93014, 1.93014, and 3.9049 l/min for the five days starting from Day 1 to Day 5, respectively. The same flow rate was repeated for Day 3 and Day 4 because this value is very close to the typical one used for solar collectors. The effect of cooling water was minimal on the temperatures of the PV3 and PV4 panels during Day 1 compared to the other days, while increasing the cooling-water flow rate decreased the average temperature of the PV3 and PV4 panels, which was affected by switching from a laminar flow scheme to a turbulent flow scheme after Day 2, according to the given water mass flow rate. The differences in the three temperatures measured for each PV panel were minimal for the reference PV (PV1) panel, while there was a noticeable difference in the remaining panels that employed the PCM, between the top and bottom ones. This was attributed to the variation in the time required to start the melting of the PCM between the top and bottom of the PCM-based panels, particularly in the PV2 panel.

The PCM played its role in controlling the panel temperatures to be mostly less than 47 °C for the PV3 and PV4 panels with the help of active cooling. However, using only the PCM effectively reduced the PV2 panel's temperature compared to the PV1 panel's temperature until noon at around 13:30 for the five days. After that, with the reduction in solar irradiance, the heat stored in the PCM along with its low thermal conductivity hampered natural cooling from taking place, which was different to what was noticed with the PV1 panel's temperature after noontime. This observation highlights the importance of coupling PV-PCM systems with active cooling or a mechanism for effective heat releasing. It is important to mention that the average inlet cooling-water temperature was 21.87 °C coming from a tank under the basement over the five days, and the minimum and maximum temperatures were 18.91 °C and 24.55 °C, respectively. This low temperature noticeably reduced the PV3 and PV4 panels' temperatures with the higher flow rate used on Day 5. The LCPV/T-PCM recorded the lowest average temperature due to the shading from the reflectors at the early and late hours of each day, and this can be noticed at 9:30 for all days in Figure 6. Generally, the average temperatures of the four PV panels over the investigated 5-day period for the PV1, PV2, PV3, and PV4 panels were 45.56, 46.29, 42.31, and 39.45 °C, respectively.

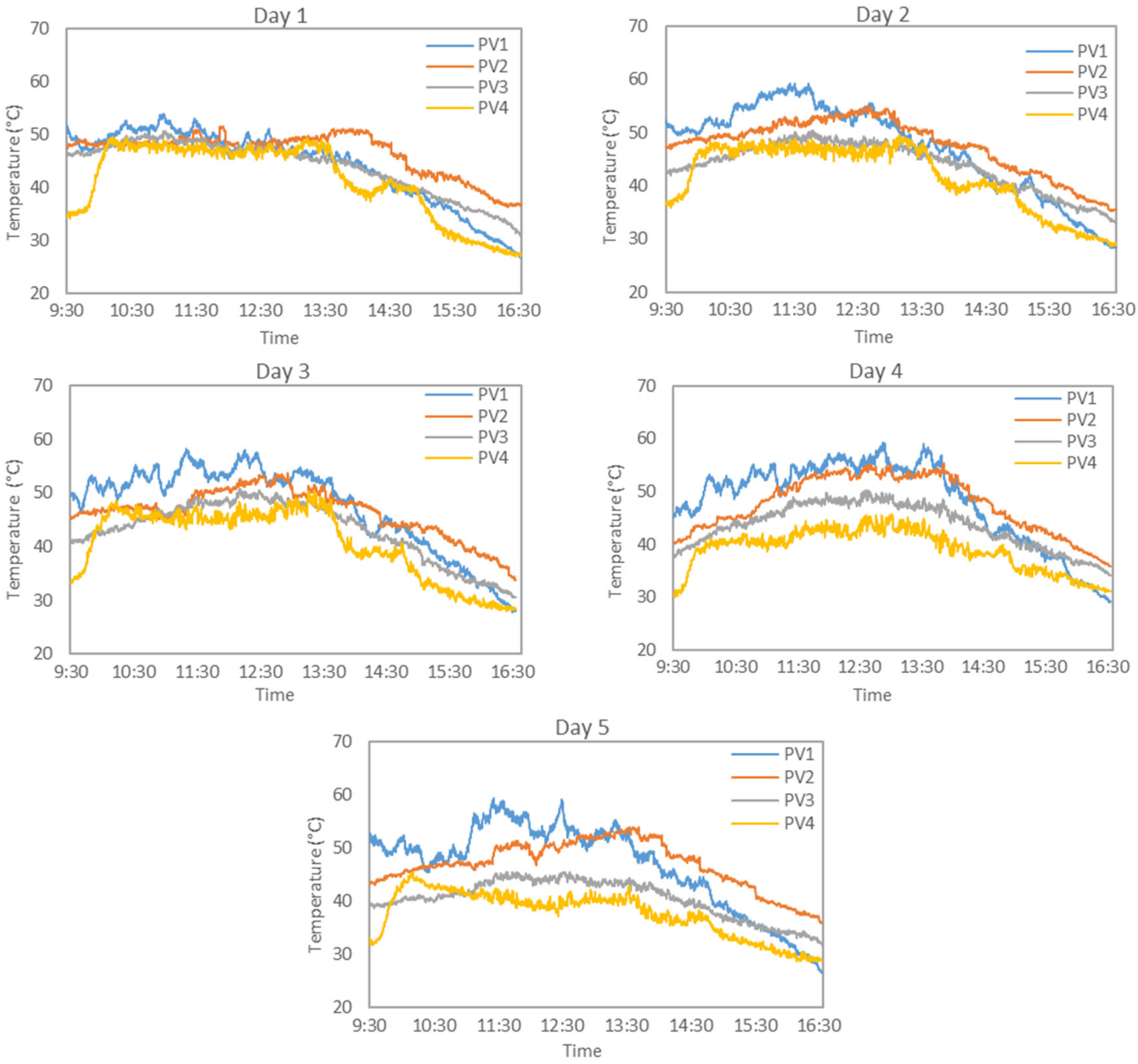

Figure 6. The average temperatures of the four PV panels measured at the back of the cells for 5 days in October 2022.

The maximum electrical power value that was recorded over the investigated 5-day period for all the PV panels is reported in Figure 7. It can be noticed that the highest electrical power was extracted from the LCPV/T- PCM system (PV4) compared to other systems, and this was only for about 2 h around noon. During these time periods, the PV4 panel produced electrical power that was, on average, 6.30% and 11.06% higher than the counterparts produced by the reference PV panel on Day 1 and Day 2, respectively. This was a direct result of using solar low-concentration system along with the combined effective cooling for the PV4 panel, and that was more pronounced on Day 5. However, in the hours outside noon times, the performance of the PV4 panel dropped dramatically due to the shading from the solar reflectors and the high dissipation of the reflected irradiance over the cells of the PV4 panel.

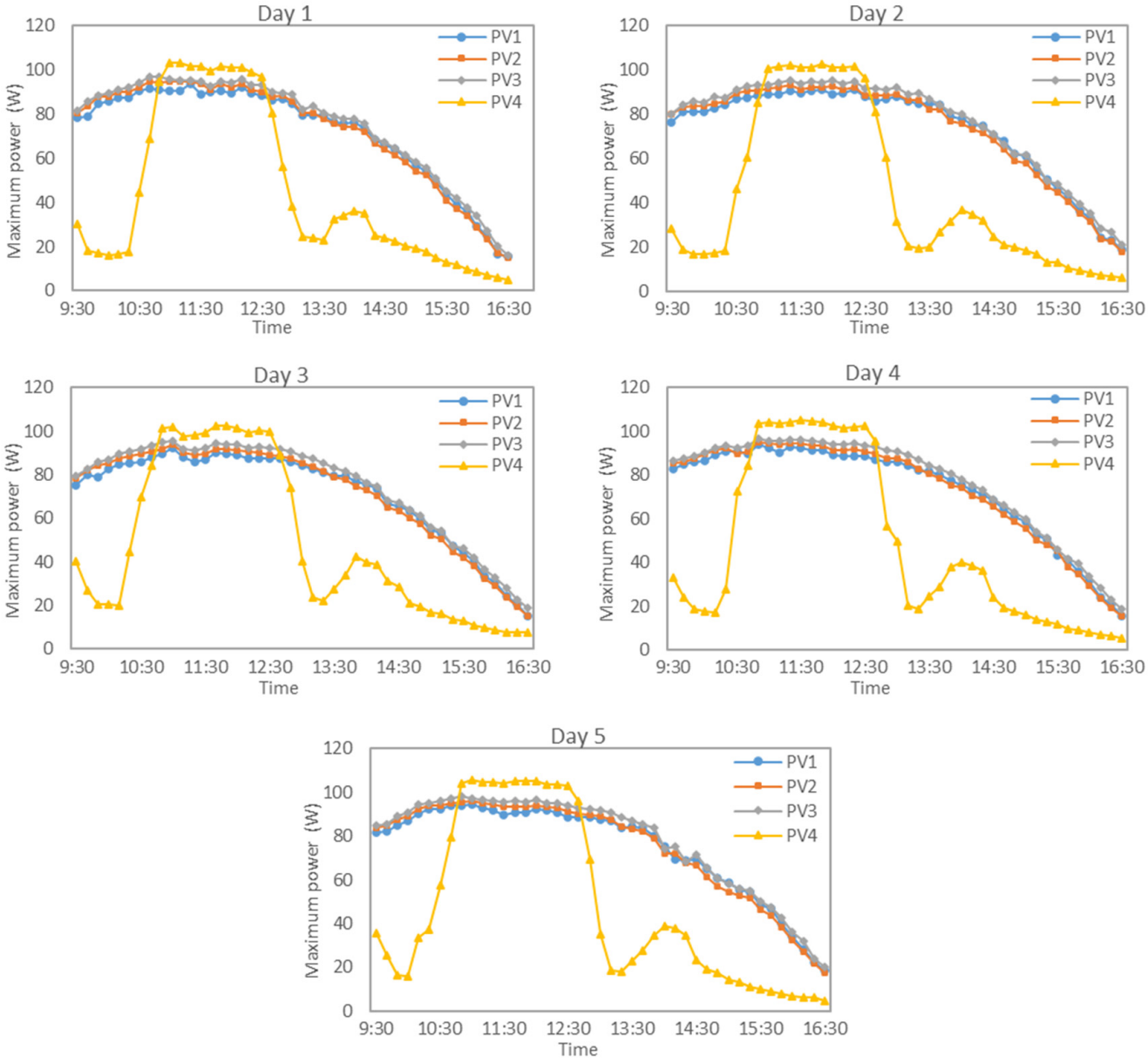

Figure 7. The maximum electrical power recorded by the PV analyzer over five days in October for the four PV panels.

Parupudi et al. [22] highlighted the importance of coupling the active cooling system when a LCPV system is applied and that can increase the power by 31% if the cell temperature is kept at 25 °C at high solar irradiance. In the present study, the average ambient temperature over the five days was 32.66 °C, while, in the summer season of Riyadh, the ambient temperature reaches 46 °C for several days with also a higher ambient temperature over the night. Therefore, the PCM melting point should be slightly higher than the expected ambient temperature over the year to perform its function in the daylight and solidify over the night. This higher temperature level prevents the PV panel in the PV-PCM system in Riyadh to work close to the standard condition of 25 °C and receive the ultimate benefits of using a solar low-concentration PV panel.

The PV/T-PCM system (PV3) showed better performance over the investigated period compared to the PV1 and PV2 systems. The average daily electrical power of the PV3 panel increased by 4.26, 4.22, 5.03, 4.50, and 3.92 % compared to the PV1 electrical power for Days 1 to 5, respectively. Despite the noticeable decrease in the temperature of the PV3

panel in comparison to that of the PV1 panel, the nonuniform temperature distribution over the relatively large surface area of the cells of the PV3 panel led to power losses. This limited further increase in the performance of the PV3 panel to higher than 5% under the investigated cases. On the other side, the PV2 panel attained a slight increase in the produced power by 0.77, 0.16, 0.61, 0.37, and 0.23% over the corresponding power produced from the reference PV panel during Days 1 to 5, respectively. The PCM used in the PV2 panel needed much more time to release the gained heat to the surrounding air in the afternoon, compared to the case of the PV1 panel. This demolished the positive effect of using the PCM when the comparison extended over an average of 7 h in the daylight under the given investigation.

The average daily electrical efficiency of the PV3 panel was recorded as the best one among the PV panels during the five days of investigation, with a maximum increase of about 5.03% on Day 3 over the efficiency of the reference PV panel. This efficiency for the PV2 panel had a negligible increase over the PV1 panel, while it declined considerably for the PV4 panel based on the average over the day, as shown in Figure 8a, where it was in the range of 8.1 to 9.17%. Over two hours at midday, the solar concentrator enhanced the PV4 panel's performance to be the best at these hours and attained a maximum average of 14.38% electrical efficiency compared to 12.94% for the PV1 panel on Day 5, as shown in Figure 8b. This can be helpful when the LCPV/T-PCM system is used to cover a higher electricity demand at this short time of the day. The LCPV/T-PCM system can provide an 11.06% increase over the conventional (reference) one if used in similar conditions to the case under study during an approximately two-hour period around noon. Otherwise, the PV/T-PCM system can represent the best choice to produce more electricity over the day combined with thermal power output. The enhancement of 5.03% in electrical efficiency of the PV/T-PCM system is consistent with what was reported in reference [15], which used only a passive cooling system with a PCM of 52 °C melting point filled in a finned container.

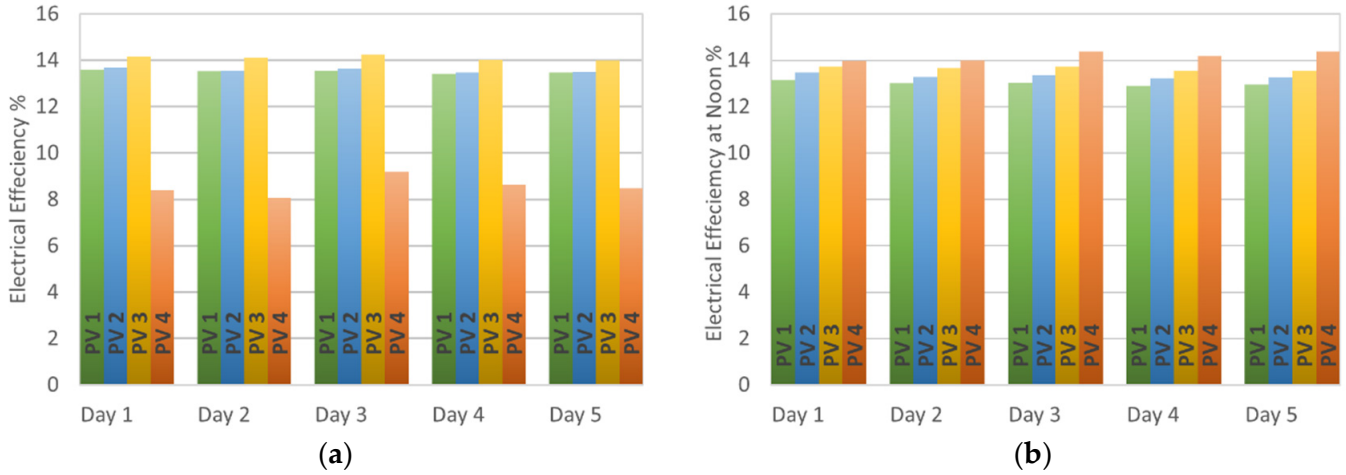

Figure 8. The average electrical efficiency of the four PV panels: (**a**) over the day from 9:30 to 16:30, and (**b**) around noon from 11:00 to 13:00.

One of the objectives of this study is to augment the overall efficiency of PV panels by utilizing them as solar collectors in PV/T systems. The effect of combining these systems with a PCM with/without solar low concentration on overall efficiency is reported in Figure 9a for the five days under the investigation. Both PV/T-PCM and LCPV/T-PCM systems showed higher average day-based overall efficiencies, attaining a maximum of 51.2% and 46.5%, respectively, on Day 4, as a result of the higher mass flow rate. Moreover, the relatively lower inlet temperature of the cooling water contributed to these higher efficiencies along with the role of the PCM in releasing the stored heat during the afternoon to the thermal fluid. This minimized the heat loss from the PV/T collector at higher solar

flux by storing the extra heat by changing the phase of the PCM and recovering it when the solar irradiance started to decline in the afternoon.

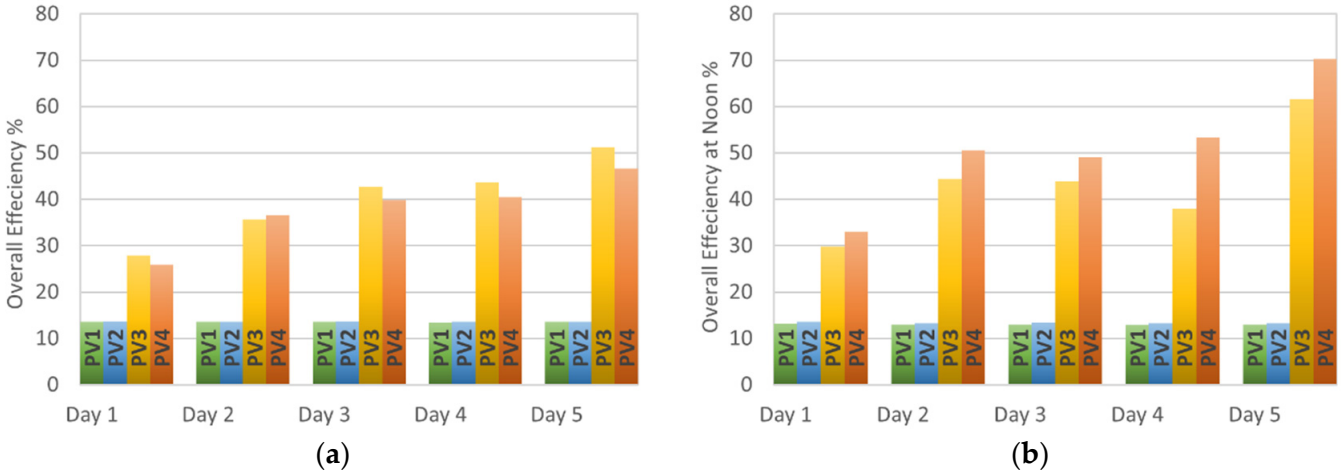

Figure 9. The average overall efficiency of the four PV panels: (**a**) over the day from 9:30 to 16:30, and (**b**) around noon from 11:00 to 13:00.

The solar low concentration magnified the thermal heat recovered from the PV4 panel at noon to reach a maximum overall efficiency of 70.3%, compared to 61.6% for the PV3 panel on Day 5, as shown in Figure 9b. The cumulative effects of low cooling-water temperature, high mass flow rate, use of the PCM, and solar low concentration contributed to reaching this higher overall efficiency.

4. Conclusions

This study reports a new experimental evaluation carried out during daylight for five days in October in Riyadh to investigate the performance of a PV-PCM, a PV/T-PCM, and a low-concentration PV/T-PCM when compared to a PV panel without cooling. The chosen PCM was Rubitherm RT-47, which has a melting temperature of 41–48 °C and is suitable for the ambient temperature of Riyadh. This study revealed that the combined passive–active cooling system, namely the PV/T-PCM, attained the best daily average electrical efficiency with 5% increase compared to the reference PV panel. The additional thermal power recovered from the PV/T-PCM brought up the overall efficiency of the PV/T-PCM to 42.7%. Coupling low solar concentration with the PV/T-PCM system was very effective for about two hours around noon, resulting in an 11% increase in electrical power, while the average electrical power over the day was the lowest. However, using the LCPV/T-PCM attained a maximum daily average overall efficiency of 46.5% on Day 5.

October is one of the best months in Riyadh in terms of higher-than-normal irradiance and moderate ambient temperatures which can lead to a good performance for a PV panel without cooling, compared to the summer season. This study reveals that, even within months beyond the severe conditions, there is a need for an efficient cooling approach to boost PV system performance. In addition, the present study shows the workability of using an active–passive cooling approach that uses a PCM with a high melting point even on off-summer days to improve the PV system performance. The solar low concentration coupled with the PV/T-PCM system needs further experimental investigations that may include different configurations and/or simple tracing systems to avoid shading effects and extend the higher-performance period.

Author Contributions: Conceptualization, M.B.E.; Methodology, M.B.E. and Z.A.; Software, S.Z. and A.A.; Validation, S.Z., O.Z., H.A. and A.A.; Formal analysis, M.B.E.; Investigation, M.B.E. and S.Z.; Resources, O.Z. and Z.A.; Data curation, S.Z., H.A. and A.A.; Writing—original draft, M.B.E. and S.Z.; Writing—review and editing, M.B.E., O.Z. and H.A.; Visualization, S.Z. and H.A.; Supervision, M.B.E. and Z.A.; Project administration, Z.A.; Funding acquisition, M.B.E. All authors have read and agreed to the published version of the manuscript.

Funding: The authors extend their appreciation to the Deputyship for Research & Innovation, "Ministry of Education" in Saudi Arabia for funding this research work through the project no. (IFKSURG-2-048).

Institutional Review Board Statement: Not applicable.

Informed Consent Statement: Not applicable.

Data Availability Statement: Not applicable.

Conflicts of Interest: The authors declare no conflict of interest.

Nomenclature

A	Area (m^2)
Cp	Specific heat (J/kg K)
D	Diameter of tube (mm)
DC	Direct Current (A)
HP	Horsepower
I	Current (A)
I	Irradiance (W/m^2)
L	Concentrator length (mm)
m	Mass flow rate (kg/s)
P	Power (W)
Re	Reynolds number
T	Temperature (°C or K)
V	Voltage (V)
Abbreviations	
ACPC	Asymmetric compound parabolic concentrator
BIPV	Building-integrated photovoltaic panel
LC	Low concentrations
LCOE	Levelized cost of energy
LCPV	Low concentrated photovoltaic
NREP	National Renewable Energy Program
PCM	Phase-change material
PV	Photovoltaic
PV/T	Photovoltaic tube/thermal
PWM	Pulse-width modulation
Greek Letters	
θ'	Internal angle
θ	External angle
η	Efficiency (%)
μ	Fluid viscosity (Pa. s)
ρ	Fluid density (kg/m^3)
Subscript	
a	Input radius
acc	LCPV acceptance angle
e	Exit
*El*ectri*c*a*l*	Electrical efficiency
i	Inlet
*ma*x	Maximum power
o*u*t	LCPV output angle
*Ov*era*ll*	Overall efficiency
r	Exit radius

References

1. Soummane, S.; Ghersi, F. Projecting Saudi sectoral electricity demand in 2030 using a computable general equilibrium model. *Energy Strategy Rev.* **2022**, *39*, 100787. [CrossRef]
2. Energy & Sustainability. 2022. Available online: https://www.vision2030.gov.sa/thekingdom/explore/energy/ (accessed on 6 May 2022).
3. Energy, G. Thermal Power will Lead Saudi Arabia Electricity Till 2030 Despite Renewables Growth. 2021. Available online: https://www.power-technology.com/comment/thermal-power-saudi-arabia/ (accessed on 7 September 2021).
4. Almasoud, A.H.; Gandayh, H. Future of solar energy in Saudi Arabia. *J. King Saud Univ.-Eng. Sci.* **2014**, *27*, 153–157. [CrossRef]
5. Radziemska, E. The effect of temperature on the power drop in crystalline silicon solar cells. *Renew. Energy* **2003**, *28*, 1–12. [CrossRef]
6. Makki, A.; Omer, S.; Sabir, H. Advancements in hybrid photovoltaic systems for enhanced solar cells performance. *Renew. Sustain. Energy Rev.* **2014**, *41*, 658–684. [CrossRef]
7. Ma, T.; Yang, H.; Zhang, Y.; Lu, L.; Wang, X. Using phase change materials in photovoltaic systems for thermal regulation and electrical efficiency improvement: A review and outlook. *Renew. Sustain. Energy Rev.* **2015**, *43*, 1273–1284. [CrossRef]
8. Stropnik, R.; Stritih, U. Increasing the efficiency of PV panel with the use of PCM. *Renew. Energy* **2016**, *97*, 671–679. [CrossRef]
9. Rajvikram, M.; Leoponraj, S.; Ramkumar, S.; Akshaya, H.; Dheeraj, A. Experimental investigation on the abasement of operating temperature in solar photovoltaic panel using PCM and aluminium. *Sol. Energy* **2019**, *188*, 327–338. [CrossRef]
10. Senthil Kumar, K.; Ashwin Kumar, H.; Gowtham, P.; Hari Selva Kumar, S.; Hari Sudhan, R. Experimental analysis and increasing the energy efficiency of PV cell with nano-PCM (calcium carbonate, silicon carbide, copper). *Mater. Today Proc.* **2021**, *37*, 1221–1225. [CrossRef]
11. Nada, S.A.; El-Nagar, D.H.; Hussein, H.M.S. Improving the thermal regulation and efficiency enhancement of PCM-Integrated PV modules using nano particles. *Energy Convers. Manag.* **2018**, *166*, 735–743. [CrossRef]
12. Mousavi Baygi, S.R.; Sadrameli, S.M. Thermal management of photovoltaic solar cells using polyethylene glycol 1000 (PEG1000) as a phase change material. *Therm. Sci. Eng. Prog.* **2018**, *5*, 405–411. [CrossRef]
13. Luo, Z.; Huang, Z.; Xie, N.; Gao, X.; Xu, T.; Fang, Y.; Zhang, Z. Numerical and experimental study on temperature control of solar panels with form-stable paraffin/expanded graphite composite PCM. *Energy Convers. Manag.* **2017**, *149*, 416–423. [CrossRef]
14. Arıcı, M.; Bilgin, F.; Nižetić, S.; Papadopoulos, A.M. Phase change material based cooling of photovoltaic panel: A simplified numerical model for the optimization of the phase change material layer and general economic evaluation. *J. Clean. Prod.* **2018**, *189*, 738–745. [CrossRef]
15. Wongwuttanasatian, T.; Sarikarin, T.; Suksri, A. Performance enhancement of a photovoltaic module by passive cooling using phase change material in a finned container heat sink. *Sol. Energy* **2020**, *195*, 47–53. [CrossRef]
16. Karthick, A.; Murugavel, K.K.; Ramanan, P. Performance enhancement of a building-integrated photovoltaic module using phase change material. *Energy* **2018**, *142*, 803–812. [CrossRef]
17. Khanna, S.; Reddy, K.S.; Mallick, T.K. Optimization of solar photovoltaic system integrated with phase change material. *Sol. Energy* **2018**, *163*, 591–599. [CrossRef]
18. Yang, X.; Sun, L.; Yuan, Y.; Zhao, X.; Cao, X. Experimental investigation on performance comparison of PV/T-PCM system and PV/T system. *Renew. Energy* **2018**, *119*, 152–159. [CrossRef]
19. Elsheniti, M.B.; Hemedah, M.A.; Sorour, M.M.; El-Maghlany, W.M. Novel enhanced conduction model for predicting performance of a PV panel cooled by PCM. *Energy Convers. Manag.* **2020**, *205*, 112456. [CrossRef]
20. Bahaidarah, H.M.S. Experimental performance evaluation and modeling of jet impingement cooling for thermal management of photovoltaics. *Sol. Energy* **2016**, *135*, 605–617. [CrossRef]
21. Teo, H.G.; Lee, P.S.; Hawlader, M.N.A. An active cooling system for photovoltaic modules. *Appl. Energy* **2012**, *90*, 309–315. [CrossRef]
22. Parupudi, R.V.; Singh, H.; Kolokotroni, M. Low Concentrating Photovoltaics (LCPV) for buildings and their performance analyses. *Appl. Energy* **2020**, *279*, 115839. [CrossRef]
23. Elsheniti, M.B.; Elbessomy, M.O.; Wagdy, K.; Elsamni, O.A.; Elewa, M.M. Augmenting the distillate water flux of sweeping gas membrane distillation using turbulators: A numerical investigation. *Case Stud. Therm. Eng.* **2021**, *26*, 101180. [CrossRef]
24. Solar, M. Maysun Solar 120W MS120M-36. Available online: https://www.maysunsolar.com/all-products/ (accessed on 5 February 2022).
25. El-Sharkawy, I.I.; AbdelMeguid, H.; Saha, B.B. Towards an optimal performance of adsorption chillers: Reallocation of adsorption/desorption cycle times. *Int. J. Heat Mass Transf.* **2013**, *63*, 171–182. [CrossRef]
26. EURONET. EURONET PWM Solar Controller. Available online: https://www.euronetdxb.com/controllers-1 (accessed on 11 February 2022).
27. OMB DAQ-56. Available online: https://assets.omega.com/manuals/M3174.pdf (accessed on 20 February 2022).
28. Besantek. BST-TP01 Thermocouples. Available online: https://www.testequipmentdepot.com/besantek/pdfs/bsttp_datasheet.pdf (accessed on 25 January 2022).
29. Sensor, H.T. Hukseflux Pyranometer. Available online: https://www.hukseflux.com/uploads/inline/LP02_manual_v2008_DISCONTINUED.pdf (accessed on 16 February 2022).

30. FLUKE87. Multimeter Datasheet. Available online: https://docs.rs-online.com/11a2/0900766b815556a4.pdf (accessed on 2 March 2022).
31. 200A, P. PV Analyzer PROVA-200A Datasheet. Available online: https://www.prova.com.tw/img/download/200A-Data%20Sheet-2015.pdf (accessed on 14 March 2022).
32. Niazmand, H.; Talebian, H.; Mahdavikhah, M. Bed geometrical specifications effects on the performance of silica/water adsorption chillers. *Int. J. Refrig.* **2012**, *35*, 2261–2274. [CrossRef]
33. Winston, R.; Miñano, J.C.; Benitez, P.G. *Nonimaging Optics*; Elsevier: Amsterdam, The Netherlands, 2005.
34. Carmona, M.; Palacio Bastos, A.; García, J.D. Experimental evaluation of a hybrid photovoltaic and thermal solar energy collector with integrated phase change material (PVT-PCM) in comparison with a traditional photovoltaic (PV) module. *Renew. Energy* **2021**, *172*, 680–696. [CrossRef]
35. He, W.; Zhang, Y.; Ji, J. Comparative experiment study on photovoltaic and thermal solar system under natural circulation of water. *Appl. Therm. Eng.* **2011**, *31*, 3369–3376. [CrossRef]
36. Holman, J.P. *Experimental Methods for Engineers*, 8th ed.; McGraw-Hill Series in Mechanical Engineering; McGraw-Hill: New York, NY, USA, 2011.